Journal of Fluorescence, Vol. 7, No. 1, 1997

Heterogeneous Photobleaching in Confocal Microscopy

Patric Van Oostveldt[1,3] and Frank Verhaegen[2]

Received June 14, 1996; accepted November 5, 1996

Photobleaching was studied during recording of confocal scanning laser microscopy. Studies on fluorescent gels of FITC-labeled dextran were used to evaluate differential bleaching along the *z*-axis. Differential bleaching along the *z*-axis was observed and it was seen that this was related to the numerical aperture of the objective in use. This points to the conclusion that photon energy flux density is an important parameter in photobleaching. To check if photon energy flux density heterogeneity is affected by local variation in the refractive index of the sample, photobleaching rates were calculated for different fluorescent objects (sections of seeds, animal cells stained with nuclear stains, immunocytochemistry preparations) and a pronounced similarity was found between photobleaching rates and DIC images.

KEY WORDS: Photobleaching; fading; confocal microscopy; fluorescence microscopy.

INTRODUCTION

Photobleaching is defined as the irreversible disappearance of the fluorescence intensity of a fluorochrome through irradiation. This phenomenon can be followed as a function of time and is frequently supposed to be a first-order kinetic at least during an initial state.[1,2,3] The information obtained from photobleaching is different from the fluorescence lifetime, which describes the time a fluorochrome is present in an excited state.[4] While fluorescence lifetime is based on a reversible phenomenon and gives an estimate of equilibrium constants between different excited states and the ground state of the fluorochrome, photobleaching is the result of an alternative pathway of the fluorochrome to part with the absorbed energy. It can be supposed that not every excited state of a single fluorochrome has the same photobleaching rate and therefore the observed photobleaching rate will be dependent on the concentration equilibrium between different excited states, which result in a deviation of simple first-order bleaching kinetics.[1] Discussing photobleaching in terms of energy, we have to define the following concepts: the energy passing through a point or photon energy flux density, with dimension $J \cdot m^{-2} \cdot s^{-1}$; the photon energy fluence ($J \cdot m^{-2}$); photon fluence ($photons \cdot m^{-2}$); and photon flux density ($photons \cdot m^{-2} \cdot s^{-1}$). As the equilibrium between excited- and ground-state molecules is determined by the photon energy flux density and the fluorescence lifetime of these different states, photobleaching will be changed according to the concentration of the different states and their photostability. In this way images can be calculated plotting photobleaching kinetics in a similar way as images of fluorescence lifetime.

More complex photobleaching can be expected if intermolecular reactions are involved. In this case, deviation from first-order kinetics can be expected, and if which molecules participate in the intermolecular reactions accompanying photodestruction can be tested, we may expect that photobleaching as well as fluorescence lifetime imaging will give valuable information on the physical and chemical environment of the fluorochrome.[5] The photodestruction or photobleaching, how-

[1] Laboratorium Biochemie en Moleculaire Cytology, Coupure Links 653, B 9000, Gent, Belgium.
[2] Laboratory for Biomedical Physics, Proeftuinstraat 86, Gent, Belgium.
[3] To whom correspondence should be addressed.

1053-0509/97/0300-0059$12.50/0

ever, will be more complex, as it can be expected to depend on the light intensity and fluorochrome concentration, and it will be more difficult to set up experiments with appropriate internal standards.

If quantitative fluorescence intensity evaluation is aimed in a confocal scanning laser microscope, knowledge of the photobleaching rate is necessary to correct for the loss of fluorescence intensity occurring during scanning of the object before the recording of the fluorescence is realized. This problem of photobleaching correction has been discussed by Rigaut and Vassy,[6] and was solved rather pragmatically by supposing a homogeneous bleaching over the whole preparation, without taking small or large heterogeneities into consideration. The approach proposed by Rigaut and Vassy,[6] furthermore, is not applicable if the distribution of fluorescent objects in the sampled volume is not random.

A main factor affecting photobleaching is the intensity of the excitation light, and therefore if photobleaching images are calculated, the even excitation of the object is a prerequisite. If the laser intensity is stable and if scanning rates are constant, we may suppose that all voxels in the object receive the same amount of light during recording of 3D confocal images. Voxels outside the detected images plane, although not visualized at that time, receive the same amount of light as imaged voxels and therefore will show proportional photobleaching. It is supposed that out-of-focus points, situated farther away from the focal plane, receive a lower intensity than points at the tip of the illumination cone, but due to the fact that they are irradiated for a longer period of time, they finally will receive the same amount of energy. However, recent[1] results indicate that photobleaching cannot be described by first-order reactions alone but is also determined by intra- and intermolecular reactions with different rate constants. Under more or less saturating conditions fast and slow conversions occur, resulting in changed steady-state concentrations of the fluorochrome, which is not a simple first-order reaction and therefore one can postulate that photobleaching is dependent not only on photon energy fluence but also on photon energy flux density. A point at the focal plane, which receives all its excitation energy in a much shorter time period, can display different photobleaching than an equivalent point outside the focal plane, which receives its excitation energy spread out over a longer period.[7]

On the other hand, heterogeneous excitation can occur if differences in refractive index in the object are present. Refractive index differences will cause lens-like effects and concentrate or diverge the excitation cone. This will cause increased or decreased excitation but is not necessarily detected as changes in emission intensities. For epiillumination fluorescence emission follows exactly the same path as excitation but in the inverse way. A positive lens converging the excitation intensity at the focal plane will diverge the emission intensity in a proportional way. Therefore an increased excitation will then be compensated by decreased fluorescence due to the same lens effect acting in the inverse way. However, photobleaching rates, which are dependent only on the excitation intensity will be affected by these differences in refractive index.

In this paper we present results of photobleaching experiments on different objects and show the effect of different heterogeneities in the object which will affect the photobleaching rate. We will try to use this information to gather further valuable information of the object.

MATERIALS AND METHODS

Fluorescent gels were prepared by dissolving 0.4 mg/ml FITC-labeled dextran (MW >2 MDa) in PBS (phosphate-buffered saline; 0.15 *M* NaCl, 0.012 *M* phosphate buffer, pH 6.8) solidified with 2% agarose and poured in a petri dish. Part of the solidified gel was cut out and mounted with its flat side on a coverglass.

Samples of paraffin-embedded material were sectioned at 20 μm and stained with pararosaniline–Schiff (0.5%) according to standard procedures[8] and mounted in Fluormount (Gurr, Essex, UK) with a refractive index of 1.5.

Animal cell cultures were stained with FITC-labeled antibodies to the cytoplasmic components and mounted in Vectashield (Vector Laboratories) or in glycerol/DABCO-containing propidium iodide (0.5 μg/ml).

Confocal Fluorescence Microscopy and Image Processing

The Bio-Rad UVMRC-600 confocal scanning laser microscope (CSLM) system was used. This instrument is equipped with two laser sources, a krypton–argon laser and a high-intensity argon-ion laser and two detection channels. The laser scanning system was mounted on a Nikon (Diaphot 300) inverted microscope. Differential interference contrast images were recorded by collecting the transmitted laser light and guiding it by an optical fiber to the second detection channel. The blue

high-sensitivity (BHS) narrow-band excitation filter from Bio- Rad was used for excitation with the 488 nm Ar^+-ion line. The krypton–argon laser in combination with the specific filters (K1 and K2) was used to observe FITC/propidium iodide signals or the pararosaniline Feulgen-stained sections. An Olympus S-plan Apo 60× oil-immersion objective lens (60×) with a numerical aperture of 1.4 or a Nikon Fluor 40 × NA 1.3–0.8 was used.

Bleaching times of 2 to 3 min were obtained by recording 12 to 24 images which are the mean of 10 to 30 frames. The FITC–dextran gels were analyzed with the 488 line of the Ar^+-ion laser confocal microscope (Bio-Rad UVMRC600) and photobleaching was recorded with the COMOS image acquisition software. Image processing was done with semper6.plus.

RESULTS

The Effect of the Numerical Aperture on Photobleaching Along the z Axis

During scanning in a confocal microscope the focused voxel will receive an equal amount of energy as out-of-focus voxels. The difference between focused voxels and out-of-focus voxels is the photon flux density, which is maximal for voxels situated in the focal plane. Out-of-focus voxels receive the same integrated excitation energy but at a lower photon flux density. During scanning, an in-focus voxel is excited by short, high-intensity light pulses. If the voxel moves out of focus, the photon energy fluence decreases but the pulse length increases proportionally. The result is that every voxel receives the same amount of integrated energy irrespective of whether it is focused or not, if we neglect the effects at the border. If photobleaching in a laser scanning confocal microscope is dependent of the photon energy flux density, we can look at the photobleaching in a homogeneous stained gels of FITC-labeled dextran and change the width of the excitation cone by altering the numerical aperture of the objective. At high numerical apertures, the excitation light cone is more obtuse and the photon energy flux density changes along the optical axis are more pronounced. Reducing the aperture of the objective will change the shape of the excitation cone and alter the photon energy flux density along the optical axis.

To evaluate an effect of the aperture on the photobleaching in the *x,z* direction, we followed the photobleaching in a homogeneously stained gel of FITC–dextran. This sample shows clear and stable photobleaching because no redistribution of the fluorochrome due to diffusion occurs. We took an image of the gel at a depth of about 25 μm below the surface with a zoom of 4. The photobleaching was induced by scanning at high intensity for about 1 min. After this experiment, the zoom was reduced to 1 and a single *x,z* image was recorded through the bleached and the nonbleached part of the gel. Figure 1 gives the *x,z* profiles along the *z* axis obtained with a single objective with an adaptable numerical aperture. It is shown in Fig. 1 that differential bleaching occurs along the *z* axis and that this is more pronounced at NA = 1.3 than at NA = 0.8. This means that higher photon flux densities induce faster photodestruction. As the photobleaching along the *z* axis is dependent of the photon energy flux density, a simple zero-order relationship cannot describe photobleaching or photodestruction.

Photobleaching of Biological Samples

If we like to use photobleaching rates to evaluate the chemical environment of the fluorochrome, it is essential to have a homogeneous excitation. A homogeneous fluorescence does not necessarily guarantee a homogeneous excitation. If refractive index differences are present, they will cause lens-like effects and can induce differences in excitation energy at the object level. These changed excitation intensities will induce differential photobleaching but are not always detected as heterogeneous fluorescence emission. Indeed, with conventional epifluorescence the emission rays follow the same path as the excitation rays, and if the excitation rays are diverged or converged by lens-like effects of overlaid refractive structures, causing local variations of the excitation energy, the emitted light is propagated exactly in the inverse way. Thus the increased or reduced local excitation can be annihilated by a decreased or increased recorded emission.

Phase-contrast images are the result of differences in refractive index within the biological samples. If photobleaching rates are caused by differential excitation of the objects, which in its turn is due to differences in the refractive index of the object or the mounting medium, we expect an analogy between photobleaching rates and phase-contrast differences. To test this hypothesis we estimated photobleaching rates for every pixel in a stack of images obtained by scanning an object at a single focal plane for consecutive times. Photobleaching rates were obtained by fitting a linear regression ($Y = bX + a$) with least-squares methods between the gray level (Y)

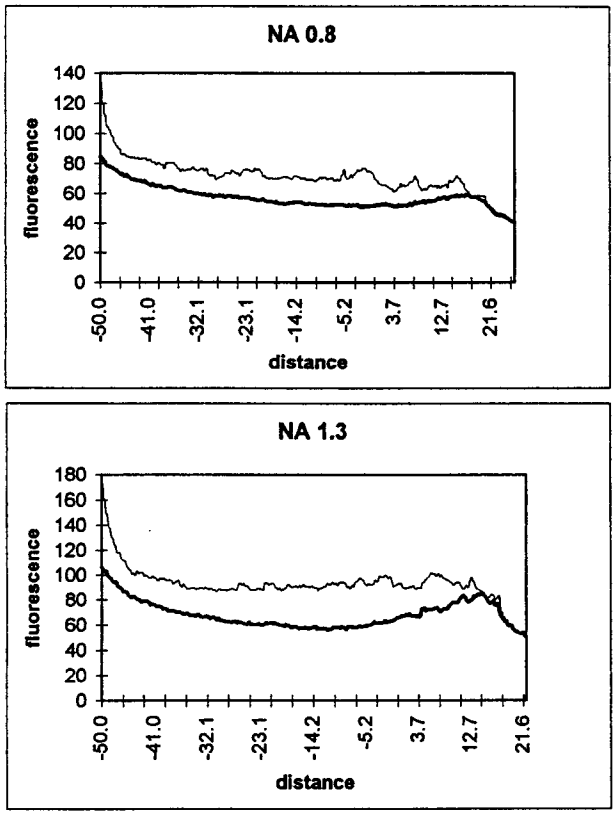

Fig. 1. Fluorescence intensity profile along the z axis of a gel bleached at focus level 0. Fine lines, profile through the nonbleached part of the gel: thick line, profile through the bleached part. (A) Using the objective lens with numerical aperture at 0.8 and (B) at 1.3. Objective NIKON Fluor 40, NA 0.8–1.3.

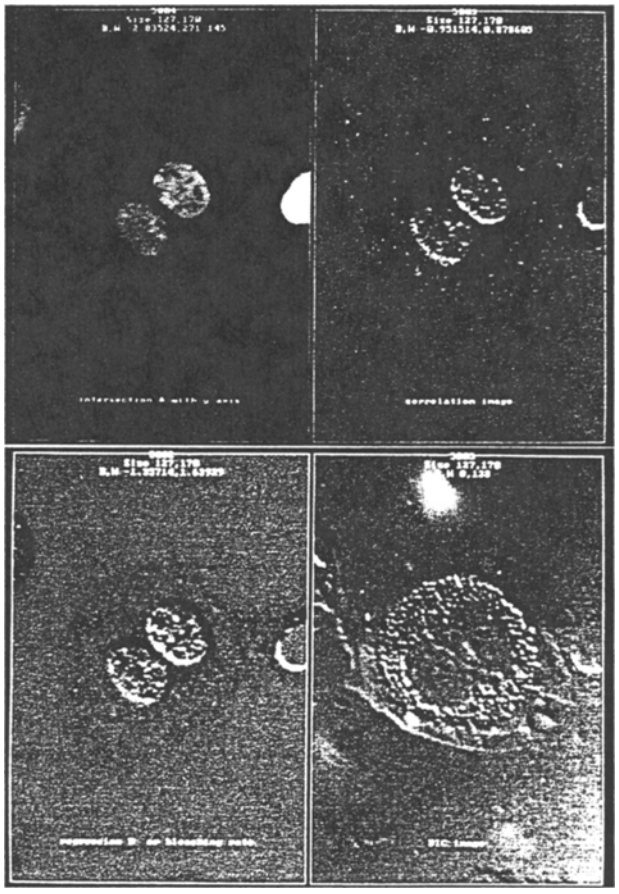

Fig. 2. Calculated images of propidiumiodide-stained cells (SKBR3 cells) compared to the DIC images. (A) Calculated image from the intersection with the y axis; (B) correlation image; (C) calculated regression of the linear fit as an estimate of the bleaching rate; (D) DIC image.

at the point x,y and the sequence number (X) of the image. Photobleaching rates were calculated for different dyes and objects recorded under different conditions and a calculated image of the photobleaching rate was directly compared with a differential interference phase-contrast image.

Having calculated the regression of fluorescence (Y) versus sequence (X), we can also calculate an image a, the intersection with the vertical axis for the linear regression $Y = bX + a$, that represents the fluorescence intensity at sequence 0 ($X = 0$). This should resemble the first fluorescent image recorded from the stack. In a similar way we constructed an image representing the regression b, which corresponds with the bleaching rate for every pixel (x,y) in the time sequence X. Finally, we calculate an image representing the correlation coefficients for every pixel. If a decrease in Y (fluorescence intensity) is correlated with an increase in X (time), $r < 0$; $r \approx 0$ if the fluorescence intensity does not change significantly with time; and $r > 0$ if fluorescence intensity increases as a function of time. In Fig. 2, the correlation image represents a gray scale where black corresponds to -1 and white to $+0.87$. If $r \approx 0$ for a pixel, it is represented as gray. This is the case for the background where no fluorescence is present. The correlation image thus shows the significance of the bleaching rate image (Fig. 2, "regression image").

A set of different calculated regression or bleaching rate images was obtained in this way and clearly shows a relation with the DIC image (Fig. 2). Some structures observed in these calculated images clearly show an increased contrast at the edge of the object as common in DIC images. Two photobleaching rate images of one object, recorded at two emission wavelengths (Fig. 3), show analogous results. If bright fluorescent objects are visualized, a pronounced contrast is seen at the edge of these objects. Figure 4 represents such a case of cells

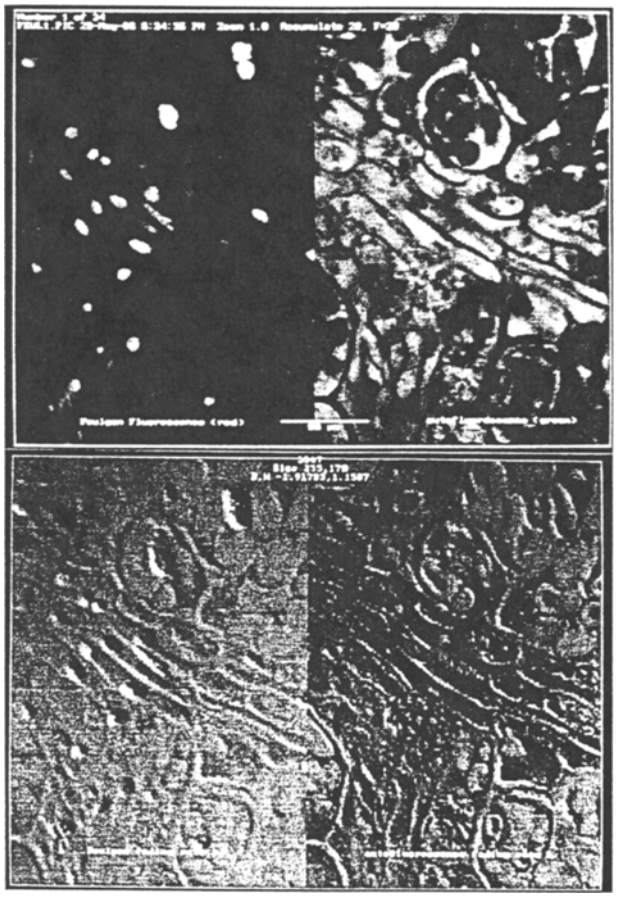

Fig. 3. Images obtained from Feulgen-stained paraffin sections of seed of pea (*Pisum sativum*). Left, red Feulgen–pararosaniline fluorescence of nucleus; right, green autofluorescence recognized as background. (A) The original fluorescent image. (B) The calculated regression for the *x,y* pixels after bleaching the object for 3 min and 10 s.

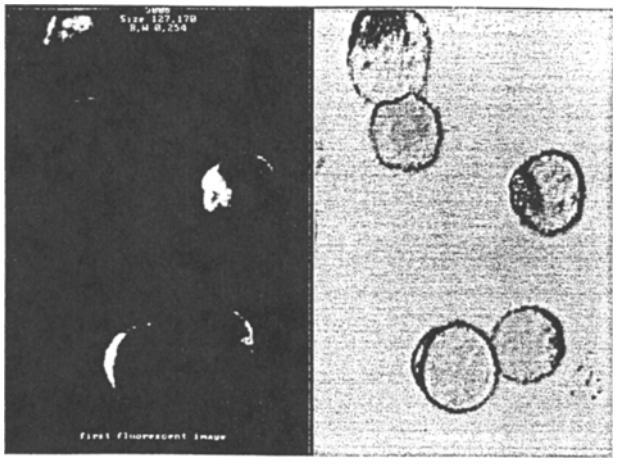

Fig. 4. Images obtained from virus-infected cells showing capping of the antigen at the cell surface. Left, the fluorescence image; right, the photobleaching rate image.

expressing a specific antigen on their surface and showing a typical capping phenomenon. The brightly stained cap shows a pronounced photobleaching which delineates the fluorescence cap or the cellular membrane.

DISCUSSION

We showed in this paper that photobleaching or photodestruction of a fluorochrome in a confocal scanning laser microscope is dependent on the photon energy flux density and is heterogeneous due to differences in refractive index caused by lens-like effects of the mounting medium or the cytoplasm. Homogeneously stained gels of FITC-labeled dextran show a differential photobleaching along the optical axis, which is influenced by the numerical aperture of the objective. These effects are seen under prolonged irradiation ($\pm$ 1 min) and therefore will not be seen if redistribution of the fluorochrome occurs during photobleaching. Small molecules, e.g., propidiumiodide, cannot be seen by these methods unless they are immobilized by absorption to large molecules, e.g., nucleic acids.

Photobleaching rates calculated for the pixels in images of biological samples (Figs. 2–4) show a pronounced variation which could be due to heterogeneous excitation. It is hypothesized that this heterogeneous excitation originates from a lens-like effect of the mounting medium around the cells or the fluorescent objects. This hypothesis is supported by the fact that the photobleaching rate image shows similarities with a differential interference contrast image. If photobleaching is accompanied by chemical reactions with nonfluorescent molecules, e.g., oxygen, we also can expect more pronounced bleaching at the border of the fluorescent object where a main zone of interaction between the fluorochrome and the oxygen will occur. At high fluorochrome concentrations therefore a differential bleaching not necessarily points to heterogeneity in the refractive index of the object. If intermolecular interactions occur during photodegradation, concentration-dependent photobleaching will occur which cannot be described by simple first-order kinetics. It can be considered therefore to calculate more complex regressions and, in this way, differentiate the kind of molecules that are engaged in this higher-order reaction.

Selective bleaching at the edge of the fluorescent objects was also reported by Brakenhoff *et al.*[9] but without mentioning a possible effect of the refractive index. Careful examination of the bleaching rate along the edges in some cases (Figs. 2 and 3) reveals a systematic uneven distribution. Instability and a systematic

shift of the scanning system relative to the object could generate a similar phenomenon. Although this cannot be excluded for a single image, repetitive controls of the instrument do not show such a systematic error in scanning or a specific translation of the object perpendicular to the optical axis. A possible explanation for this phenomenon could be the incomplete symmetry of excitation and emission light path due to small differences in the orientation of the optical axis for excitation and emission. This can be induced by mechanical errors, an inappropriate alignment of the mirrors, and a small inclination of the object table relative to the optical axis but also some systematic aberration induced by the coverslip on the object.

It is known that mismatches of the refractive index of the mounting medium can affect resolution and distance measurements in a confocal microscope.[10,11] Our results indicate that fairly small refractive index differences create differential photobleaching that is caused by altered photon energy flux density.

ACKNOWLEDGMENTS

Serge Bauwens for stimulating discussion, Herman Favoreel for the virus-infected cells, and Chris De Potter and Elisabeth Coene for SKBR3 cells. The FKFO and the NFWO are acknowledged for grants to P.V.O.

REFERENCES

1. L. Song, E. J. Hennink, I. T. Young, and H. J. Tanke (1995) *Biophys. J.* **68**, 2588–2600.
2. T. M. Jovin, D. J. Arndt-Jovin, G. Marriott, R. M. Clegg, M. Robert-Nicoud, and T. Schorman (1990) in B. Herman and K. Jacobson (Eds.), *Optical Microscopy for Biology*, Wiley–Liss, New York, pp. 575–602.
3. W. W. Webb, K. S. Wells, D. R. Sandison, and J. Strickler (1990) in B. Herman and K. Jacobson (Eds.), *Optical Microscopy for Biology*, Wiley–Liss, New York, pp. 73–108.
4. A. Draaijer, R. Sanders, and H. C. Gerritsen (1995) in J. Pawley (Ed.), *Handbook of Biological Confocal Microscopy*, 2nd ed., Plenum Press, New York, pp. 491–505.
5. H. Brismar, O. Trepte, and B. Ulfhake (1995) *J. Histochem. Cytochem.* **43**, 699–707.
6. J. P. Rigaut and J. Vassy (1991) *Anal. Quant. Cytol. Histol.* **13**, 223–232.
7. R. Y. Tsien and A. Waggoner (1995) in J. Pawley (Ed.), *Handbook of Biological Confocal Microscopy*, 2nd ed., Plenum Press, New York, pp. 267–279.
8. P. Van Oostveldt and R. Van Parijs (1976) *Exp. Cell Res.* **98**, 210–221.
9. G. J. Brakenhoff, K. Visscher, and E. J. Gijsbers (1994) *J. Microsc.* **175**, 154–161.
10. S. Hell, G. Reiner, C. Cremer, and E. H. K. Stelzer (1993) *J. Microsc.* **169**, 391–405.
11. T. D. Visser, J. L. Oud, and G. J. Brakenhoff (1992) *Optik* **90**, 17–19.